Marine Chemistry 190 (2017) 1–12

Contents lists available at ScienceDirect

Marine Chemistry

journal homepage: www.elsevier.com/locate/marchem

Distribution of transparent exopolymer particles (TEP) across an organic carbon gradient in the western North Atlantic Ocean

Meredith K. Jennings [a,*], Uta Passow [b], Andrew S. Wozniak [c], Dennis A. Hansell [a]

[a] Department of Ocean Sciences, Rosenstiel School of Marine and Atmospheric Science, University of Miami, Miami, FL 33149, USA
[b] Marine Science Institute, University of California Santa Barbara, Santa Barbara, CA 93106, USA
[c] Department of Chemistry and Biochemistry, Old Dominion University, Norfolk, VA 23529, USA

ARTICLE INFO

Article history:
Received 20 June 2016
Received in revised form 23 November 2016
Accepted 15 January 2017
Available online 17 January 2017

Keywords:
TEP
TOC
Organic matter
Western North Atlantic Ocean
Sea surface microlayer
Phytoplankton bloom
Subtropical gyre

ABSTRACT

In this study, the abundance of transparent exopolymer particles (TEP) is examined across a surface water gradient of organic carbon from a phytoplankton bloom region in the western North Atlantic to oligotrophic waters in the Sargasso Sea, including a coastal region sampled near Cape Cod. TEP are macrogels that reach up to millimeters in size and abiotically assemble from dissolved acidic polysaccharides secreted by phytoplankton. Due to their great stickiness, TEP self aggregate and also form aggregates with non-TEP particulate organic carbon (POC). Aggregation enhances ballasting, thereby mutually facilitating export and subsequent sedimentation of both TEP and POC, increasing the efficiency of the biological pump. Here, four distinct regions with varying chlorophyll *a* concentrations, temperature, and salinity were sampled in the upper column, at the surface, and from the sea surface microlayer (SML). While TEP in seawater shows no correlation to chlorophyll *a*, nutrients, or total organic carbon (TOC) concentration, a strong correlation exists between TEP and TOC in the SML; and concentrations of both variables are inversely proportional to surface productivity as indicated by chlorophyll *a* concentrations. As open ocean regions show greater enrichments of TEP and TOC in the SML compared to the coastal region, we suggest that the role of the SML in organic carbon cycling is dependent on regional biogeochemistry and productivity. We hypothesize that a lower abundance of particles in oligotrophic regions compared to bloom regions limits TEP export by sinking, thus increasing the residence time of TEP in the upper water column and the SML.

1. Introduction

Transparent exopolymer particles (TEP) are surface active macrogels that play a role in the marine carbon cycle by spanning the size continuum between dissolved and particulate organic carbon (DOC and POC, respectively), in addition to supporting particle aggregation (Alldredge et al., 1993; Passow, 2002a; Verdugo et al., 2004). TEP are operationally defined as transparent particles stainable with Alcian Blue, a dye that preferentially binds to acidic polysaccharides by complexing with half-ester sulfate and carboxyl groups (Alldredge et al., 1993; Passow and Alldredge, 1995). TEP abiotically assemble from dissolved polysaccharides produced by phytoplankton (Logan et al., 1995; Passow, 2002a; Thuy et al., 2015). As TEP have surface-active properties and are neutrally buoyant, they are easily scavenged by rising bubbles and concentrated at the air-sea interface, thereby contributing appreciably to the organics in the sea surface microlayer (SML) (Azetsu-Scott and Passow, 2004; Cunliffe et al., 2013; Mopper et al., 1995; Wurl et al., 2009).

TEP formation and distribution are controlled by a combination of regional physical and biological factors, including wind-induced turbulence, salinity, and production of dissolved polysaccharide precursors by phytoplankton and bacteria. Nutrient levels control phytoplankton composition, which is one of the underlying factors that mediate the partitioning of organic matter between dissolved and particulate phases (Carlson et al., 1998; Conan et al., 2007; Lomas and Bates, 2004; Thornton, 2014), and production of TEP and organic matter (Claquin et al., 2008; Corzo et al., 2000; Mari et al., 2005; Passow, 2002b). TEP-chlorophyll *a* (Chl-*a*) relationships exist during the development of a bloom, reflecting the production of TEP by phytoplankton (Passow, 2002a). However, the relationship between Chl-*a* and TEP during bloom development is species-specific, with the cellular production rate of TEP by phytoplankton affected by their growth phase. Therefore, no overall TEP–Chl-*a* relationship would be expected along a spatial gradient where different phytoplankton taxa exist at different life stages. Nutrient limitation often increases TEP production, but also

* Corresponding author.
E-mail addresses: meredith.jennings@rsmas.miami.edu (M.K. Jennings), uta.passow@lifesci.ucsb.edu (U. Passow), awozniak@odu.edu (A.S. Wozniak), dhansell@rsmas.miami.edu (D.A. Hansell).

http://dx.doi.org/10.1016/j.marchem.2017.01.002
0304-4203/

may impede bacterial consumption of TEP (Bar-Zeev and Rahav, 2015), allowing TEP to accumulate and aggregate as C-rich N-poor organic material in surface waters (Passow, 2002a).

Elevated concentrations and formation rates of gel particles have been observed in the SML (Orellana et al., 2011; Wurl et al., 2011a), indicating the importance of gels for carbon cycling at the air-sea interface. Low density, surface active material (such as TEP) is transferred to the SML after absorbing to rising bubbles created by breaking waves (Wurl et al., 2011b; Wurl and Holmes, 2008). Although these breaking waves temporarily disperse its components into underlying waters, the SML has a rapid reformation rate (Cunliffe et al., 2013). Through bubble bursting, biogenic material concentrated in the SML may also be introduced to the atmosphere as components of sea spray aerosols (SSA) capable of cloud condensation and ice nucleation (Bigg and Leck, 2008; DeMott et al., 2015; Orellana et al., 2011; Quinn et al., 2014; Wang et al., 2015; Wilson et al., 2015). Since TEP adhere to rising bubbles (Mopper et al., 1995) and are enriched in the SML, TEP could contribute to the organic enrichment of sea spray aerosols derived from film droplets (Aller et al., 2005).

TEP are often 1–2 orders of magnitude stickier than non-TEP particles, acting as a glue to promote aggregate formation of particles and subsequently enhance sedimentation (Logan et al., 1995; Passow et al., 1994). If TEP are ballasted by particles with adequate density (such as large phytoplankton or mineral dust aggregates), TEP and the associated particles will be stripped from surface waters (Azetsu-Scott and Passow, 2004). As TEP and POC sink in the water column, they provide a source of carbon to the deep ocean as microbial hotspots. Although sinking mechanisms of marine aggregates have been investigated (Burd and Jackson, 2009; Iversen and Robert, 2015; Jokulsdottir and Archer, 2016; Prairie et al., 2015), there remains the need to understand the role of TEP in the biological carbon pump (Burd et al., 2016; Zetsche and Ploug, 2015).

More comprehensive analyses of TEP distributions that include SML measurements are required to better describe the role of TEP in the carbon cycle as a particulate sink for DOC and dynamic component of total organic carbon (TOC). Here, we assess TEP and TOC concentrations within the upper water column, the surface layer, and SML across biogeochemical gradients to evaluate the potential sources and impacts of TEP accumulation in the coastal and open ocean.

2. Methods

2.1. Study areas

Samples were collected during the Western Atlantic Climate Study II (WACS2) field campaign conducted May 20 to June 5, 2014 onboard the RV *Knorr* (Cruise KN219). The cruise stations encompassed four hydrographically distinct areas along Chl-*a*, sea surface temperature (SST) and sea surface salinity (SSS) gradients. These areas, designated as A) *Slope Water*, B) *Gulf Stream*, C) *Sargasso Sea*, and D) *Coastal* regions, ranged from a phytoplankton bloom located between the Scotian Shelf and the Gulf Stream (*Slope Water*; 42.5°N, 61.5°W) to an oligotrophic region near Bermuda (*Sargasso Sea*; 33.5°N, 63°W), and including an intermediate region (*Gulf Stream*; 40°N, 62°W) and a station off the coast of Cape Cod (*Coastal*; 40.5°N, 70.5°W) (Fig. 1). The entire study area encompassed a spectrum of end-members from lower salinity coastal water to higher salinity open ocean seawater, from subpolar to subtropical temperature ranges, and eutrophic to oligotrophic status, which influence the biogeochemistry of carbon and nutrients. Further hydrographic complexities are present in the intermediate region as it captures the meandering of the Gulf Stream.

2.2. Sampling

Seawater samples were collected from the upper 200 m of the water column, from the surface layer, and from the SML. Water column samples were collected on 9 casts (2 in region A, 4 in region B, 2 in region C, and 1 in region D; Fig. 1) using clean 12 L Niskin bottles attached to a conductivity temperature depth (CTD) rosette (Sea-bird SBE-911plus). Water column sample collection was evenly distributed from the surface to 200 m for TOC and nutrient analyses (~5–10 depths per cast) and TEP analyses (~4–8 depths per cast). Surface water samples ($n = 12$) were collected by lowering a clean 5 L polypropylene bucket to approximately 1 m depth, recovering onto the deck, and immediately transferring to a 9-L polycarbonate carboy for subsequent sampling for TOC, TEP, and POC. SML samples ($n = 3$) were obtained using the 'Interface II', a battery operated and remote controlled catamaran sampler containing a rotating drum coated in a thin layer of hydrophilic Teflon film (Knulst et al., 2003) that collected SML material for TOC and TEP analysis into an amber glass bottle. The SML in region C was not sampled due to prohibitive wind and sea conditions. Surface water and SML samples were collected near the ship, as the sampling devices were required to be tethered. Samples for nutrient ($n = 36$) and Chl-*a* ($n = 138$) analyses were continuously collected from the ship's underway sample line (intake at ~5 m depth) such that collections were evenly distributed throughout the cruise track.

2.3. Sample analysis

2.3.1. Temperature, salinity, and wind speed

Underway temperature and salinity were measured using the ship's thermosalinograph (Sea-Bird SBE-45), while the conductivity and temperature sensors packaged on the CTD rosette were used for upper water column samples (Sea-bird SBE-911plus). Mixed layer depth was estimated as the depth in the water column where the vertical change in potential density was >0.01 kg m^{-3}. Potential density was calculated from the temperature and salinity of continuous CTD profiles averaged to 1-m bins. Wind speed was measured from the ship's meteorological instrumentation (Vaisala WXT520) and averaged to 1-minute intervals.

2.3.2. Chlorophyll a

Chl-*a* concentrations (Fig. 1) were taken from NASA MODIS AQUA 9-km Products 8 day composite (17 May–24 May 2014) and visualized with Ocean Data View software (Schlitzer, 2015). Discrete fluorometric Chl-*a* samples were collected from the ship's underway seawater line into well-rinsed 500 mL amber Nalgene bottles and gently vacuum filtered (<5 mmHg) onto 25 mm GF/F filters (Whatman; 0.7 μm nominal pore size). Samples were extracted into 7 mL 100% methanol for 24 h in the dark at −20 °C and read on a Turner Designs 10 AU fluorometer calibrated with a commercial Chlorophyll-*a* standard (Sigma) and checked against a solid standard daily.

2.3.3. Nutrients

Samples were collected directly into HDPE bottles and stored frozen (for phosphate and combined nitrate and nitrite samples) or at 4 °C (for silicic acid samples) until analysis post-cruise (no later than 3 months). Concentrations of combined nitrate and nitrite ($NO_3^- + NO_2^-$) were first reduced to NO using a heated, acidic vanadium (III) solution and determined in duplicate by chemiluminescent detection of NO (Braman and Hendrix, 1989) using KNO_3 as a standard. Analyses of phosphate (PO_4^{3-}) and silicic acid (SiO_4^{4-}) followed standard methods established by Grasshoff (1976) and Strickland and Parsons (1972), respectively. Both phosphate and silicic acid were determined colorimetrically following using a spectrophotometer (Shimadzu UV-1800) with KPO_4 and silicic acid certified material (www.osil.co.uk) as standards.

2.3.4. Total organic carbon

Water column, surface, and SML samples were collected unfiltered into acid washed 60 mL polycarbonate bottles and stored frozen until analysis post-cruise at the University of Miami. TOC was measured in triplicate injections by high temperature combustion using a Shimadzu TOC-L auto analyzer (CV = 1.5 to 2.5%) following methods from

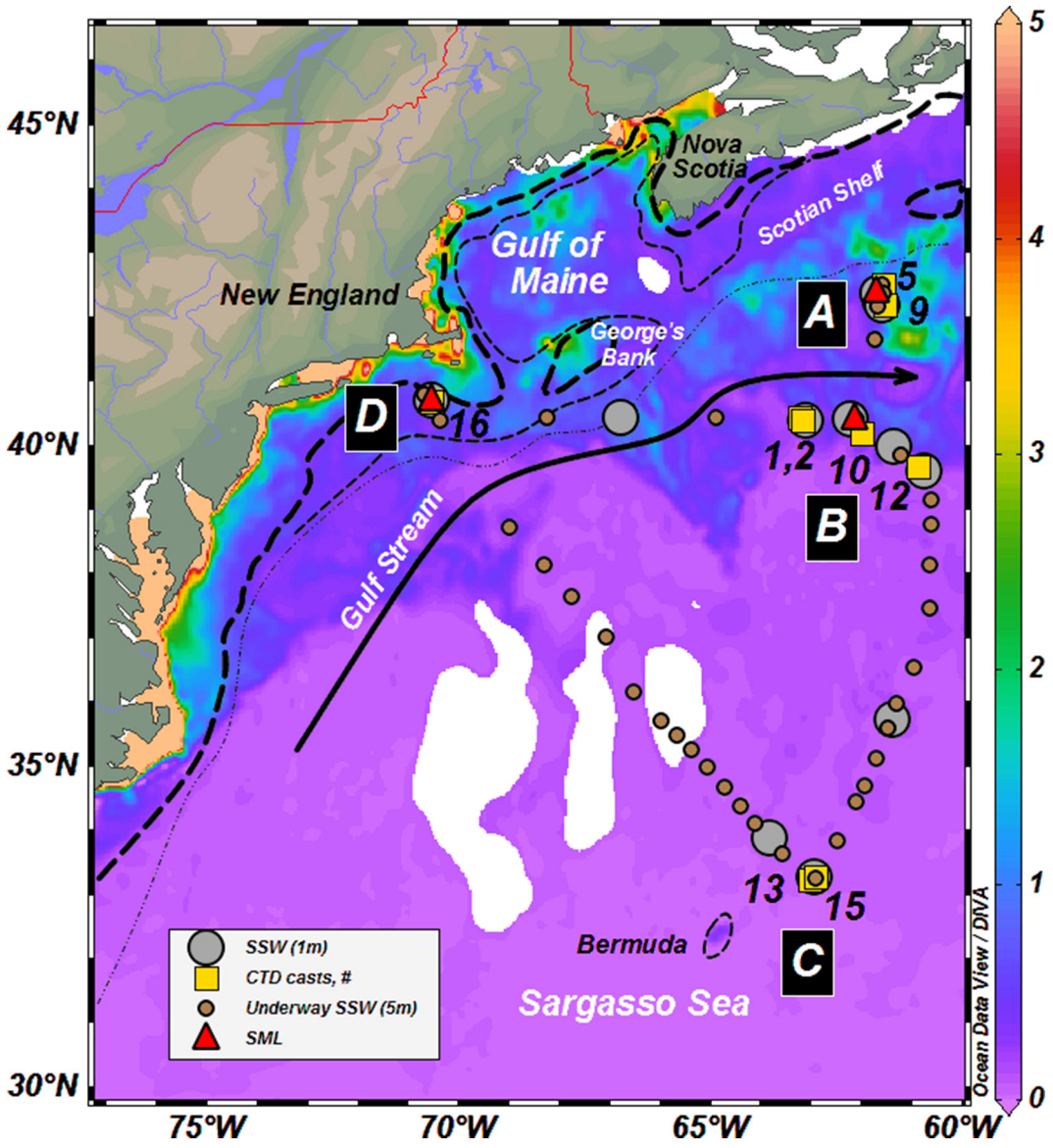

Fig. 1. Hydrographic stations of WACS2 cruise, sampled during May and June 2014 in the western North Atlantic Ocean, Sargasso Sea, and off the coast of New England. Chlorophyll *a* concentrations (background color; mg m^{-3}) during 17 May–24 May 2014 were taken from NASA MODIS AQUA 9-km Products 8 day composite. Boxes A–C represent open ocean stations distinguished as Slope Water (A), Gulf Stream (B), and Sargasso Sea (C); Box D represents a shallow, coastal station on the southern New England shelf (referred to as Coastal). The symbols represent types of samples collected for TOC and TEP concentration, i.e. surface samples (grey circles), water column CTD samples (yellow squares, labeled by cast number), and surface microlayer samples (red triangles). Smaller brown circles represent locations where underway nutrients were sampled along the cruise track. The curved arrow details the approximate location of the Gulf Stream where a temperature difference of nearly 10 °C was observed. Dotted and dashed lines represent the bathymetry of the continental shelf. (For interpretation of the references to color in this figure legend, the reader is referred to the web version of this article.)

Dickson et al. (2007) and quality controlled using consensus reference materials (Hansell, 2005).

2.3.5. Particulate organic carbon

Surface seawater was subsampled (500 mL) directly in-line from a 9 L polycarbonate carboy and filtered through pre-combusted (450 °C) glass fiber filters (Whatman; 0.7 μm nominal pore size) using a polycarbonate filter holder (Pall; 47 mm diameter); the material remaining on the filter was retained for measurement of POC. Inorganic carbonates were removed from the samples by acidification with 1 M HCl and the samples dried in a drying oven (60 °C, 24 h) prior to analysis. Portions of the acidified filters were placed in 5 × 9 mm tin cups and combusted at 900 °C in the presence of O_2 and measured on a CE Elantech Flash EA 1112 elemental analyzer in duplicate analyses. Sample response areas were calibrated to a standard curve generated with an aspartic acid standard.

2.3.6. Transparent exopolymer particles

TEP was collected from the upper water column by subsampling directly from the Niskin bottle into 1 L HDPE bottles, from the surface water by subsampling directly from a 9 L polycarbonate carboy (following POC collection), and from the SML by subsampling from a secondary polycarbonate container into 60 mL polycarbonate bottles. Samples were either filtered immediately after collection or stored at 4 °C prior to filtration (no later than 24 h after collection). Samples were filtered in triplicate using 0.4 μm (and also 0.2 μm for SML samples, surface samples, and casts 1, 2, 9, 13, 16) pore size 25 mm polycarbonate filters (Whatman Nuclepore), stained with 0.5 mL Alcian Blue solution (pH = 2; 0.16% w/v Alcian Blue 8GX, Sigma) calibrated with Gum Xanthan (Sigma) by the Passow Lab at the University of California Santa Barbara, and frozen onboard (Passow and Alldredge, 1995). The volume of water necessary for each TEP analysis varied from 10 mL collected from the SML to 1000 mL collected from the maximum depth

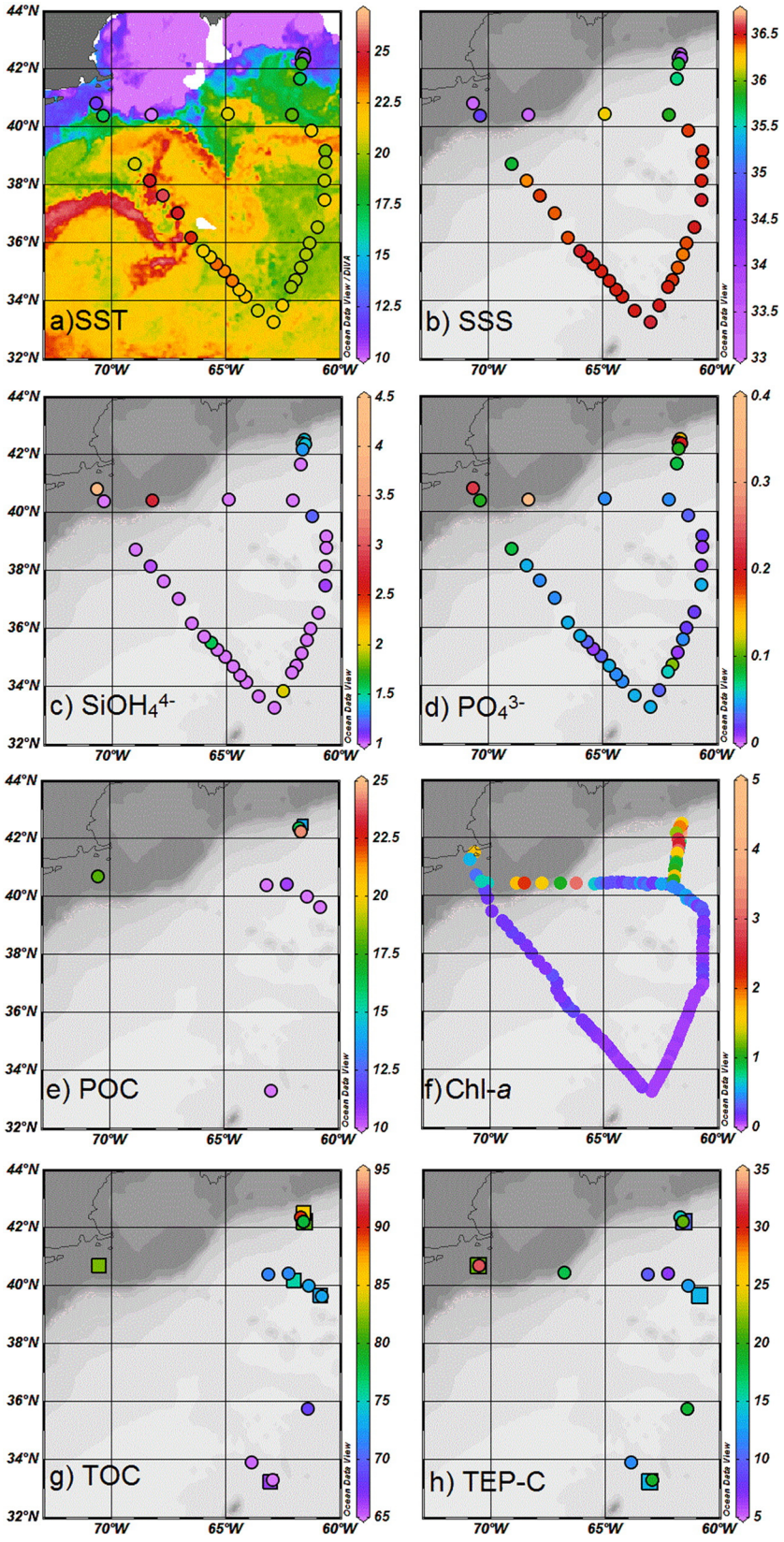

Fig. 2. Surface water measurements of a) sea surface temperature (SST; °C), b) sea surface salinity (SSS), c) silicic acid (μmol SiO_4^{4-} L^{-1}), d) phosphate (μmol PO_4^{3-} L^{-1}), e) POC (μmol L^{-1}), f) fluorometric chlorophyll *a* (μg Chl-*a* L^{-1}), g) TOC (μmol L^{-1}), and h) TEP-C (μmol L^{-1}) larger than 0.4 μm collected from ~1 m depth. Measurements are shown in color. Symbols represent samples collected from underway/surface bucket sampling (circles) and from surface CTD niskin bottles (squares). Background color of a) is satellite SST during 17 May–24 May 2014 taken from NASA MODIS AQUA 9-km Products 8 day composite, while the background of b)–h) is bathymetry from the standard map resource in Ocean Data View software. (For interpretation of the references to color in this figure legend, the reader is referred to the web version of this article.)

sampled in the water column (e.g., 200 m), depending on the general concentration of particles in the sample. Ideally, enough seawater was filtered from each depth to measure TEP concentrations well above the detection limit, while avoiding seawater volumes that would clog the filter with extraneous non-TEP particles.

Post-cruise, the Alcian Blue stain was extracted from sample filters in 80% H_2SO_4 and analyzed for UV absorption at 787 nm using a spectrophotometer (Shimadzu UV-1800). As the dye binds to acidic groups, this method is semi-quantitative when the chemical composition of TEP is unknown. The concentration of TEP was determined in units of Gum Xanthan equivalents per volume sampled, or μg Xeq. L^{-1}.

For the majority of our analyses, we report only the concentration of TEP collected using the 0.4 μm filters in order to provide comparison to most literature values. When both 0.2 μm and 0.4 μm pore sizes were used (SML samples, surface samples, and samples from casts 1, 2, 9, 13, 16), the 0.2 μm filters retained on average 37% more TEP than the 0.4 μm filters (SD = 16.7%), similar to the 42% higher retention differential reported by Sun et al. (2012). By sampling with both filter sizes, we assessed the size spectrum exhibited by TEP.

2.4. Derived values

2.4.1. TEP carbon unit conversion

To simplify comparisons of TEP to TOC and POC, the concentration of TEP (collected on both 0.2 and 0.4 μm filters) was converted from units of μg Xeq. L^{-1} to units of TEP carbon (μmol TEP-C L^{-1}). TEP-C conversion factors depend on the chemical composition of TEP and range from 0.51 to 0.88 μg TEP-C L^{-1} per μg Xeq. L^{-1} as determined experimentally from phytoplankton cultures (Engel, 2004; Engel and Passow, 2001). It is therefore important to consider our TEP-C estimates as semi-quantitative yet indicative of gradients (Filella, 2014). In this study, we used the value of 0.5 μg TEP-C L^{-1} per μg Xeq. L^{-1}, as it is expected that lower values are more appropriate under non-culture conditions and the colorimetric method for determining TEP concentration has been shown to overestimate carbon (Passow, 2002a). The following equation summarizes the unit conversion to TEP carbon (μmol TEP-C L^{-1}) from μg Xeq. L^{-1}:

$$\mu\text{mol TEP-C L}^{-1} = \mu\text{g Xeq.L}^{-1} \times \frac{0.5\ \mu\text{g TEP-C L}^{-1}}{\mu\text{g Xeq.L}^{-1}} \times \frac{\mu\text{mol TEP-C}}{12.01\ \mu\text{g TEP-C}}$$

2.4.2. Enrichment factors

Enrichment factors (EF) were calculated by dividing the TEP or TOC concentration in the SML by the concentration found in the underlying surface seawater (SSW), e.g.

$$EF = [TEP]_{SML}/[TEP]_{SSW}$$

3. Results

3.1. Regional water mass characterization

Sea surface temperature (SST) and salinity (SSS) measurements from the ship's underway seawater line help define warm Gulf Stream water and colder waters to the north marked by a sharp change in temperature (Fig. 2a, b). North of the Gulf Stream, the Slope Water region (Fig. 1, region A) had the coldest SST (~10.6 °C) and freshest SSS (~33.6) of the open ocean regions sampled along the cruise track. The cruise track captured meandering of the Gulf Stream (region B), where SST ranged from ~19.4 to ~22 °C and SSS ranged from ~35.9 to ~36.5. South of the Gulf Stream, the Sargasso Sea (region C) is identifiable by warm SST (~20.2 to ~23.4 °C) and high SSS (~36.4 to ~36.6). West of the Gulf Stream, the Coastal station (region D) was distinguished by relatively fresh (~33 to ~34.7) and cold (10 to 17 °C) surface water.

A T-S diagram of the upper 200 m of the water column supports our classifications of the four regions: Slope Water, Gulf Stream, Sargasso Sea, and Coastal (Fig. 3). Sargasso Sea waters (casts 13 and 15, blue symbols) had a narrow range and elevated salinity and temperature (36.5 to 36.6; 18.7 to 21.5 °C). Gulf Stream waters (casts 1, 2, and 10; yellow symbols) had high salinity (36.1 to 36.7) and temperature (15.8 to 21.9 °C), similar to the subtropical Sargasso Sea. Slope Water (casts 5 and 9, green symbols) was colder and fresher than subtropical waters, with a wide range of salinity (33.6 to 35.5) and a narrow range in temperature (9.8 to 13.5 °C). Cast 12 (purple triangles) is apparently a mixture between Slope Water and subtropical waters, demonstrating intermediate temperature and salinity ranges (13.9 to 21.7 °C; 35.6 to 36.4). Coastal water (cast 16, red symbols) was the freshest and coldest water sampled, with a relatively narrow range of both temperature and salinity (8.5 to 13.2 °C; 33.0 to 33.3).

Mixed layer depths (MLD) are given in Table 1. Slope Water had a shallower MLD (~16 to 18 m) than the Gulf Stream and Sargasso Sea regions (~26 to 49 m). The Coastal MLD was shallowest at ~12 m (~60 m bottom depth).

3.2. Biogeochemical parameters

3.2.1. Nutrients

The surface (5 m) distributions of silicic acid and phosphate are shown in Fig. 2c, d; combined nitrate and nitrite is not shown because it was very low (<0.9 μmol $NO_3^- + NO_2^-$ L^{-1}) or undetectable (<0.03 μmol $NO_3^- + NO_2^-$ L^{-1}) in the open ocean. The Slope Water region

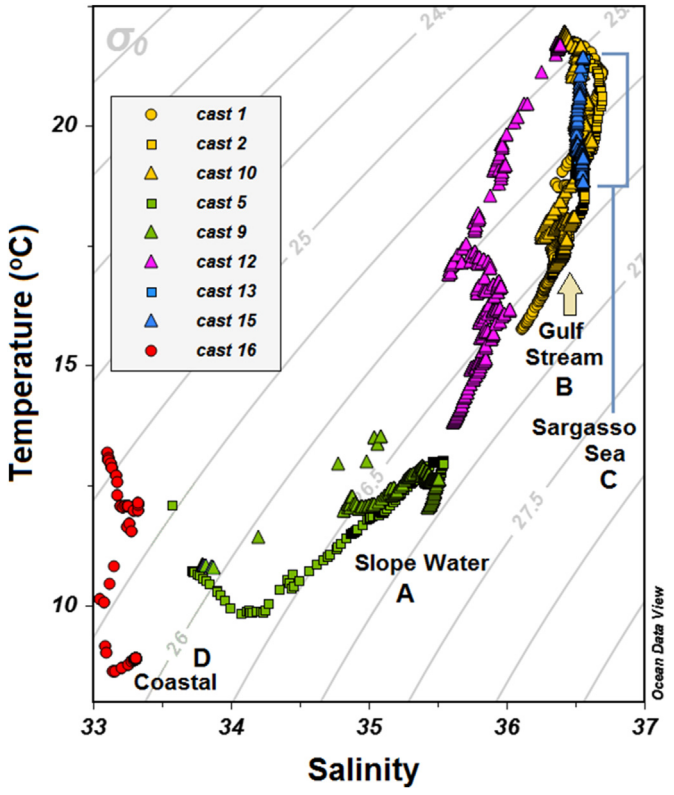

Fig. 3. Temperature-Salinity (T-S) plot of the upper 200 m of water column (in continuous 1 m bins). In the background, isopycnals are depicted as contours of constant potential density (σ_θ). Casts from each region are grouped by color: Slope Water (A, green symbols), Gulf Stream (B, yellow), Sargasso Sea (C, blue), an apparent mixture between Slope Water and subtropical waters (cast 12; purple), and Coastal (D, red). (For interpretation of the references to color in this figure legend, the reader is referred to the web version of this article.)

Table 1
Sampling dates, locations and mixed layer depths (MLD) for water column samples (200 m vertical CTD casts).

CTD cast no.	Region	Date	Lat. (°N)	Long. (°W)	MLD (m)
5	Slope Water, A	2014-05-25	42.4850	61.552	16.4
9	Slope Water, A	2014-05-27	42.1860	61.528	9.97
1 & 2	Gulf Stream, B	2014-05-22	40.4180	63.211	48.8
10	Gulf Stream, B	2014-05-28	40.1620	61.970	28.7
12	Gulf Stream, B	2014-05-30	39.6460	60.846	36.1
13	Sargasso Sea, C	2014-06-01	33.2680	62.906	35.3
15	Sargasso Sea, C	2014-06-02	33.2140	63.017	25.9
16	Coastal, D	2014-06-04	40.6740	70.534	12.1

contained elevated silicic acid and phosphate (up to 1.4 μmol SiO_4^{4-} L^{-1} and 0.2 μmol PO_4^{3-} L^{-1}), with extremely low values of combined nitrate and nitrite (<0.05 μmol $NO_3^- + NO_2^-$ L^{-1}). Silicic acid and phosphate were detectable in both Gulf Stream and Sargasso Sea waters (0.45 to 2 μmol SiO_4^{4-} L^{-1} and 0.01 to 0.11 μmol PO_4^{3-} L^{-1}). All three nutrients were highest in the Coastal region, where silicic acid ranged from 0.7 to 4.1 μmol SiO_4^{4-} L^{-1}, phosphate ranged from 0.08 to 0.37 μmol PO_4^{3-} L^{-1}, and nitrate was as high as 0.9 μmol $NO_3^- + NO_2^-$ L^{-1}.

Water column nutrient profiles for each cast (Fig. 4a) reflect surface distributions for silicic acid and phosphate (Fig. 2c–d). Nutrient concentrations in the upper water column are lower in the Gulf Stream (yellow symbols) and Sargasso Sea casts (blue symbols) (0.02 to 0.18 μmol PO_4^{3-} L^{-1}, 0.3 to 5.4 μmol SiO_4^{4-} L^{-1}, and 0 to 9.2 μmol $NO_3^- + NO_2^-$ L^{-1}) relative to the more nutrient-rich Slope Water (green symbols; 0.2 to 1.1 μmol PO_4^{3-} L^{-1}, 0 to 8.3 μmol SiO_4^{4-} L^{-1}, and 0 to 16.8 μmol $NO_3^- + NO_2^-$ L^{-1}) and the Coastal (red symbols; 0.26 to 0.65 μmol PO_4^{3-} L^{-1}, 1.2 to 8.8 μmol SiO_4^{4-} L^{-1}, and 0 to 1.1 μmol $NO_3^- + NO_2^-$ L^{-1}) casts. Nutrient concentrations of the Slope Water-subtropical mixture (cast 12; purple symbols; 0.01 to 0.6 μmol PO_4^{3-} L^{-1}, 0.7 to 3.3 μmol SiO_4^{4-} L^{-1}, and 0 to 8.7 μmol $NO_3^- + NO_2^-$ L^{-1}) fall within the ranges exhibited by Sargasso Sea and Gulf Stream casts. Nutrients increase with potential density (Fig. 4b), and Gulf Stream casts generally had the highest nutrient concentrations on a given isopycnal. Sargasso Sea water and the Slope Water-subtropical mixture (cast 12) showed great similarity.

3.2.2. Chl-a

Satellite imaging (Fig. 1) confirmed by discrete fluorometric analyses (Fig. 2f) reveals a regional gradient of surface Chl-*a* spanning three orders of magnitude, with concentrations ranging as high as 4 μg Chl-*a* L^{-1} within the bloom in the Slope Water region to as low as 0.04 μg Chl-*a* L^{-1} in the Sargasso Sea. Intermediate Chl-*a* concentrations were detected in the Gulf Stream region (~0.5 μg Chl-*a* L^{-1}) and the Coastal region (~0.7 μg Chl-*a* L^{-1}).

3.2.3. TOC

Surface (upper 1 m) TOC concentrations are shown in Fig. 2 and Table 2. A TOC gradient was observed with latitude, with the highest values in Slope Water (average 83.5 ± 5.8 μmol L^{-1}), lowest values in the Sargasso Sea (average 64.8 ± 0.4 μmol L^{-1}), and intermediate values in the Gulf Stream and Coastal regions (average 72 ± 0.8 μmol L^{-1}; 79.5 μmol L^{-1}, respectively).

TOC decreased with depth and density (Fig. 4). Spatial gradients were observed in samples from the upper 25 m (from 86 μmol L^{-1} in Slope Water to 65 μmol L^{-1} in Sargasso Sea waters), while TOC approached a unified value of 55 μmol L^{-1} deeper in the water column (~200 m) in the open ocean casts. At constant σ_θ, Gulf Stream waters had the lowest TOC, with Slope Water having the highest TOC.

TOC was elevated in the SML from each region, with values up to 4× greater than those observed in underlying waters (Fig. 5, Table 2). TOC concentrations in the SML of the Gulf Stream were highest

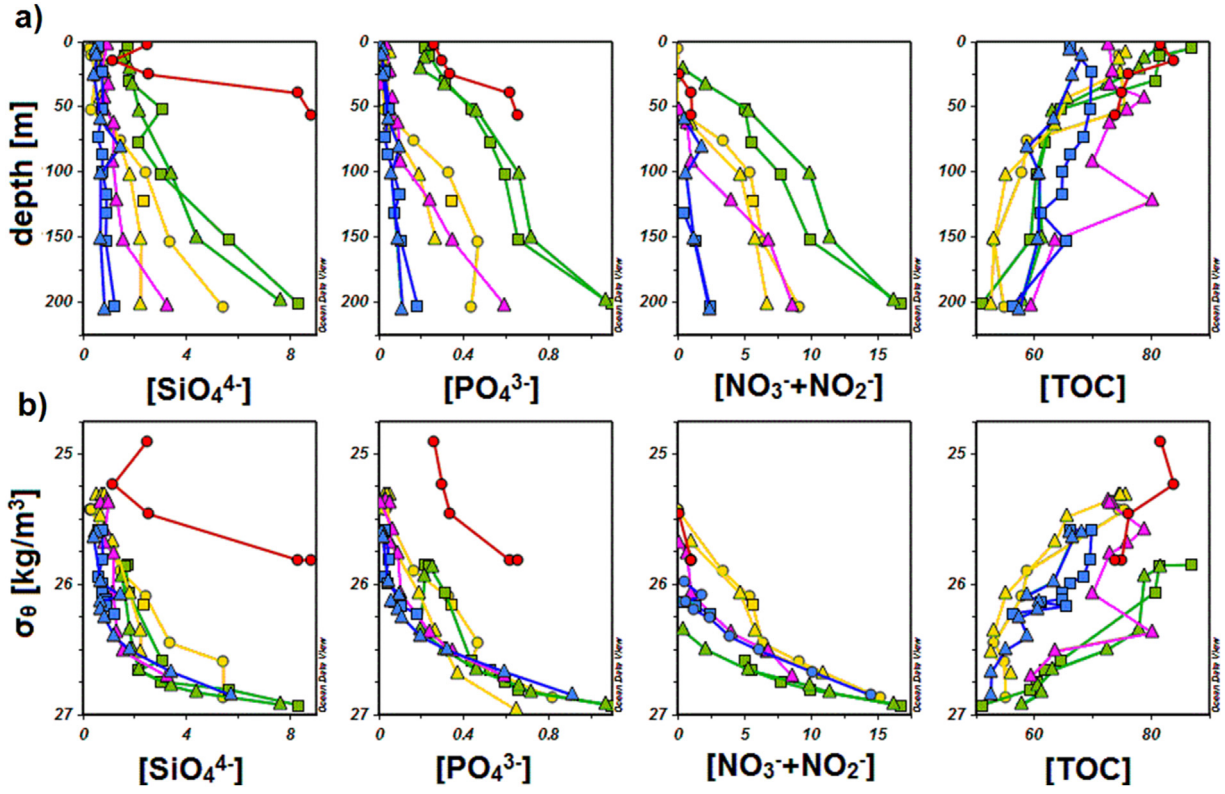

Fig. 4. Profiles of silicic acid (μmol SiO_4^{4-} L^{-1}), phosphate (μmol PO_4^{3-} L^{-1}), combined nitrate and nitrite (μmol $NO_3^- + NO_2^-$ L^{-1}) and TOC (μmol L^{-1}) concentration in upper 200 m shown with a) depth and b) increasing potential density (σ_θ). Symbols follow the same legend presented in Fig. 3 and are grouped by color: Slope Water (green symbols), Gulf Stream (yellow), Slope Water-Subtropical mixture (cast 12; purple), Sargasso Sea (blue), and Coastal (red). Combined nitrate and nitrite concentrations in the upper 50 m were below the detection limit in the Sargasso Sea and Gulf Stream regions. (For interpretation of the references to color in this figure legend, the reader is referred to the web version of this article.)

Table 2
Meta-data and results from sea surface water (SSW, upper 1 m) and sea surface microlayer (SML) samples (total organic carbon (TOC), particulate organic carbon (POC), and transparent exopolymeric particle concentration measured in units of Gum Xanthan equivalents per volume sampled, or μg Xeq. L^{-1} and estimated in units of carbon (TEP-C)) are presented for the four different regions. Derived values for percent (%) contribution of POC or TEP-C to TOC (% POC of TOC = POC/TOC × 100), enrichment factors (EF = SML/SSW_{avg}) of TEP-C and TOC in the SML, and the ratio of POC to TEP-C (POC/TEP-C) are listed. Only TEP >0.4 μm pore size is shown.

Sample ID	Date	Lat. (°N)	Long. (°W)	TOC (μmol L^{-1})	POC (μmol L^{-1})	TEP (μg Xeq. L^{-1})	TEP-C (μmol L^{-1})	% POC of TOC	% TEP-C of TOC	EF_{TEP}	EF_{TOC}	POC/TEP-C
Slope Water, A												
SML (2)	2014-05-26	42.3702	61.682	208	–	5672 ± 401	241 ± 17	–	116	13.4	2.3	–
SSW (4)	2014-05-24	42.2199	61.602	82.6	24.4 ± 0.6	392 ± 39	17 ± 2	29.5	20			1.4
SSW (5)	2014-05-26	42.3573	61.673	89.6	16.1 ± 4.4	361 ± 42	15 ± 2	18	17			1.1
SSW (6)	2014-05-27	42.1825	61.581	78.2	–	516 ± 90	22 ± 4	–	28			–
SSW_{avg}				83.5 ± 5.8	20.2 ± 5.8	423 ± 82	18 ± 3	24	22			1.1
Gulf Stream, B												
SML (1)	2014-05-23	40.3972	62.111	303	–	9549 ± 472	405 ± 20	–	134	34.2	4.2	–
SSW (2)	2014-05-22	40.3722	63.105	71.4	8.3 ± 1.8	235 ± 15	10 ± 1	12	14			0.83
SSW (3)	2014-05-23	40.4010	62.2099	71.7	10.6 ± 0.3	161 ± 8	7 ± 0.5	15	10			1.5
SSW (7)	2014-05-29	39.9632	61.3501	72.9	9.1 ± 1.0	298 ± 124	13 ± 5	12.5	17			0.7
SSW (8)	2014-05-30	39.5972	60.7344		9.5 ± 1.0	–	–	–	–			–
SSW_{avg}				72 ± 0.8	9.4 ± 1.0	279 ± 111	10 ± 3	13	14			0.9
Sargasso Sea, C												
SSW (10)	2014-06-01	33.2635	62.913	64.5	8.25 ± 1.8	460 ± 173	20 ± 7	13	30			0.4
SSW (11)	2014-06-02	33.8620	63.824	65	–	283 ± 15	15 ± 1	–	18			–
SSW_{avg}				64.8 ± 0.4	8.25 ± 1.8	372 ± 125	17.5 ± 4	13	24			0.4
Coastal, D												
SML (3)	2014-06-04	40.6831	70.526	94	–	2207 ± 203	94 ± 9	–	100	2.8	1.2	–
SSW (12)	2014-06-04	40.6831	70.526	79.5	18.2 ± 1.0	787 ± 119	33 ± 5	23	42			0.5

(303 μmol L^{-1}), compared to the SML of Slope Water (208 μmol L^{-1}) or Coastal (94 μmol L^{-1}) regions.

3.2.4. POC

Surface (upper 1 m) POC is shown in Fig. 2. Similar to TOC, a gradient of POC is observed with latitude with the highest values in Slope Water and Coastal regions (average 18.2 ± 5.5 μmol L^{-1}; 24.4 μmol L^{-1} respectively), lowest values in the Sargasso Sea (8.25 μmol L^{-1}), and intermediate values in the Gulf Stream (average 9.3 ± 1 μmol L^{-1}).

3.3. TEP-C

Average surface TEP-C concentrations (0.4 μm pore size) were lowest in the Gulf Stream region (10 ± 3 μmol L^{-1}), nearly equivalent in Slope Water and Sargasso Sea regions (18 ± 3 μmol L^{-1} and 17.5 ± 4 μmol L^{-1}, respectively), and highest in the Coastal region (33 ± 5 μmol L^{-1}) (Fig. 2f, Table 2). Concentrations were highest at the surface and decreased with depth (Fig. 6). With respect to depth, the Coastal region had higher TEP-C than any of the open ocean areas (Slope Water, Gulf Stream, Sargasso Sea) sampled. In the upper 25 m of the water column, the TEP concentrations agreed within repetitive casts per region in both Slope Water (9 ± 1 μmol L^{-1} in cast 5; 9 ± 1 μmol L^{-1} in cast 9) and Gulf Stream (9 ± 2 μmol L^{-1} in cast 1 and 9 ± 1 μmol L^{-1} in cast 10) regions, while the Sargasso Sea had more variability between casts (10 ± 4 μmol L^{-1}in cast 13; 7 ± 0 μmol L^{-1} in cast 15). Below the mixed layer (~10 m to 50 m) in the open ocean, TEP concentrations were generally lower in the Slope Water region, higher in the subtropical Gulf Stream and Sargasso Sea, and highest in cast 12 (Slope Water-Subtropical mixture). The Fig. 6 inset shows the distribution of TEP with σ_θ to demonstrate that the Coastal and Slope Waters have greater TEP concentrations than Sargasso Sea and Gulf Stream waters at the same σ_θ.

Overall, TEP was 1–2 orders of magnitude greater in the SML than in the underlying upper water column (Table 2). TEP concentrations in the SML (Fig. 5, Table 2) were highest in the Gulf Stream region (405 ± 20 μmol L^{-1} for 0.4 μm pore size and 527 ± 42 μmol L^{-1} for 0.2 μm pore size) and lowest in the Coastal region (94 ± 9 μmol L^{-1} for

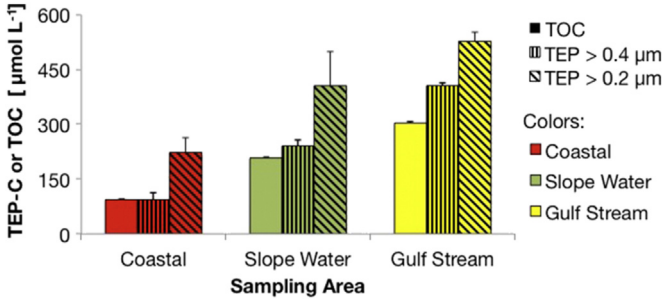

Fig. 5. Concentrations of TOC (μmol L^{-1}) (solid bars) and TEP-C > 0.4 μm (μmol L^{-1}) (vertical striped bars) and >0.2 μm (μmol L^{-1}) (diagonal striped bars) in the SML. Error bars represent the standard deviation of triplicate measurements.

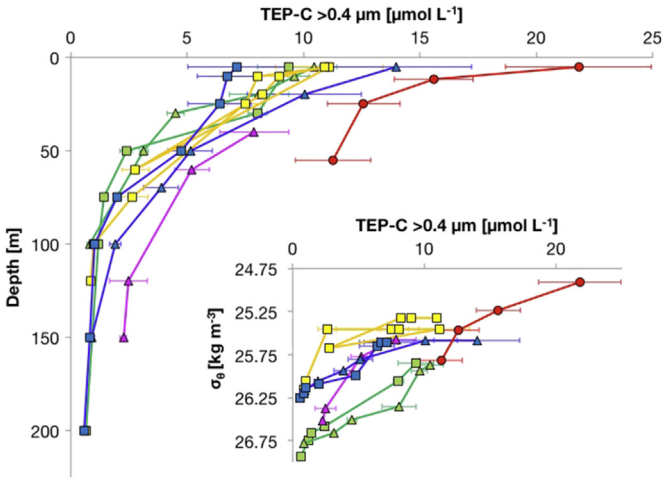

Fig. 6. Water column profiles (upper 200 m) of TEP-C > 0.4 μm (μmol L^{-1}) with depth and increasing density, σ_θ (inset). Symbols follow the same legend presented in Fig. 3 and are grouped by color: Slope Water (green symbols), Gulf Stream (yellow), Slope Water-Subtropical mixture (cast 12; purple), Sargasso Sea (blue), and Coastal (red). Error bars represent standard deviation of three replicates. (For interpretation of the references to color in this figure legend, the reader is referred to the web version of this article.)

Table 3
Contribution (%) of TEP-C to TOC throughout sea surface microlayer (SML), sea surface water (SSW), and water column for the four different regions (A–D).

Layer/region	Slope Water (A)	Slope Water-subtropical mixture (B)	Gulf Stream (subtropical) (B)	Sargasso Sea (C)	Coastal (D)
SML	116	–	134	–	100
SSW (~1 m)	22	–	14	26	42
0–10 m	12	19	9	16	27
10–50 m	8	10	10	10	16
50–100 m	2	7	3	5	–
100–200 m	1	3	2	1	–

0.4 μm and 223 ± 26 μmol L^{-1} for 0.2 μm). Falling between the two extremes, TEP in the Slope Water region SML were 241 ± 17 μmol L^{-1} for 0.4 μm and 405 ± 94 μg μmol L^{-1} for 0.2 μm.

Because we collected TEP on both 0.2 and 0.4 μm pore size filters from the SML, we were able to estimate the percentage of total TEP (larger than 0.2 μm) sized between 0.2 and 0.4 μm (i.e. smaller size fraction), or >0.4 μm (i.e. a larger size fraction). The majority of TEP in the Gulf Stream SML (~80%) and the Slope Water SML (~60%) fell within the larger size fraction (>0.4 μm). Conversely, the majority of TEP in the Coastal SML (~60%) fell within the smaller size fraction (between 0.2 and 0.4 μm).

3.4. Organic carbon partitioning and enrichments

The surface waters of the Slope Water and Coastal regions had the highest percentage of TOC as POC (24 and 23%, respectively) compared to the Gulf Stream and Sargasso Sea surface waters that each had 13% of TOC as POC (Table 2). The elevated contributions of POC to TOC in the Slope Water and Coastal regions coincided with higher concentrations of Chl-*a* (Fig. 2f).

The contribution of TEP-C to TOC was calculated in the SML, surface waters, and selected depth ranges of the water column (Table 3). TEP-C in the Gulf Stream SML contributed a greater fraction to the organic carbon pool (134%) compared to the SML sampled in the Slope Water and Coastal regions (116% and 100%, respectively). Clearly values over 100% are impossible and emphasize the semi-quantitative character of the measurements. However, such high contributions do highlight that most of the TOC in the SML of all water masses consisted of TEP. TEP contributions in surface water, in contrast, were low, with TEP-C contributing to only 14% of TOC in the Gulf Stream, 26% in the Sargasso Sea, and 22% and 42% in the Slope Water and Coastal regions, respectively. Overall, the contribution of TEP-C to TOC decreases with depth in the water column, ranging from 8% at 10–50 m to <3% at 100–200 m in the open ocean areas. The Coastal station had a shallow bottom depth of ~60 m, with TEP-C representing 16% of the TOC at its deepest depths.

The highest enrichments were observed in the Gulf Stream region (34.2- and 4.2-fold for TEP and TOC, respectively) followed by lower enrichments in the Slope Water region (13.4- and 2.3-fold, respectively; Table 2). The Coastal region SML had the lowest enrichments of TEP and TOC (2.8- and 1.2-fold fold, respectively; Table 2).

4. Discussion

We present new evidence that TEP plays a significant role in organic carbon dynamics of the surface ocean, particularly in the SML where TEP-C represented nearly 100% of TOC (Tables 2 and 3). Our TOC values agreed with previously reported measurements (Wanninkhof et al., 2013), and establish an organic carbon gradient extending from a phytoplankton bloom (higher TOC) to an oligotrophic region (lower TOC). By sampling four regions of varying productivity that encompassed a wide range of water mass characteristics, we examine the relative proportions of TEP-C to TOC, and consider which biogeochemical parameters likely control the spatial distribution of TEP concentration and enrichment. Although we did not observe a correlation between the surface distribution of TEP and nutrients, chlorophyll *a*, nor TOC concentration, we report a correlation between TEP and TOC in the SML with concentrations of both variables being inversely proportional to surface productivity as indicated by chlorophyll *a* concentrations.

A density gradient established by differences in temperature and salinity was used to classify each of the four regions (Slope Water, Gulf Stream, Sargasso Sea, and Coastal) and helped further characterize subtropical or subpolar influences. The Gulf Stream and Sargasso Sea regions are comparable based on similar subtropical temperature and salinity, nutrient depletion, and lower surface TOC and POC concentrations (Figs 1, 2, and 3). Since the SML in the Sargasso Sea was not sampled, we use the Gulf Stream as our oligotrophic reference to contrast the biologically productive Slope Water and Coastal regions that were both distinguished by colder and fresher waters containing higher TOC, POC, and nutrient concentrations. These differences in density likely also affected the settling behavior of aggregates (including TEP) as aggregate settling speeds are slowed down in waters with increased stratification (Prairie et al., 2013). Even across this diverse set of systems, a relationship between TEP and TOC is observed in the SML (Fig. 7a), and lack thereof in underlying surface waters (Fig. 7b), which further suggests that TEP is a substantial component of TOC in the SML.

4.1. TEP and TOC enrichments in the SML

The finding that TEP-C contributed to nearly all TOC in the SML, but only to a small fraction in the water below (Table 3), is consistent with the result that TEP and TOC were heavily enriched in the SML relative to underlying surface water throughout the study area. The Gulf Stream region had the highest enrichments of TEP and TOC, followed by the Slope Water region, with the lowest enrichments found in the Coastal region SML (Table 2). A similar trend of higher enrichment in the SML of open ocean versus coastal regions was observed by previous studies (Carlson, 1983; Wurl and Holmes, 2008). We further note an inverse trend with apparent productivity, as the Coastal region SML was the least concentrated and enriched in TEP and TOC (Fig. 5) and the subtropical Gulf Stream region had greater concentrations and enrichments than the more biologically productive Slope Water region. Wurl et al. (2011b) also reported greater enrichment of surfactants in the SML of oligotrophic waters versus more productive waters.

4.2. Suggested mechanisms for TEP enrichment

The greater enrichment of TEP in oligotrophic conditions likely results from multiple interactive processes, for many of which we do not have direct measurements (bacterial abundance, SML thickness and density, phytoplankton composition, particle flux, or TEP precursor concentrations) or the observed ranges were too small to be quantitatively useful. We refer to Wurl et al. (2011a) for a comprehensive conceptual model of TEP cycling in the ocean and a discussion of biogeochemical drivers of TEP production and fate. This model describes the primary source of TEP in surface waters as aggregates of dissolved polysaccharides that were either directly exuded from phytoplankton or biproducts of grazing or viral lysis. Once formed, TEP adsorb to bubbles and enrich the microlayer where they are exposed to UV radiation, which physically destroys the TEP and stimulates microbial consumption of TEP. TEP may be distributed throughout the water column and SML, while undergoing several cycles of lysis, grazing, and aggregation. Because TEP are neutrally buoyant, they are capable of both ascending and descending depending on environmental circumstances, the presence or absence of ballasting particles, or act of scavenging by rising bubbles. However, here we will specifically investigate the role of non-gel organic particle concentrations in providing a ballast for TEP

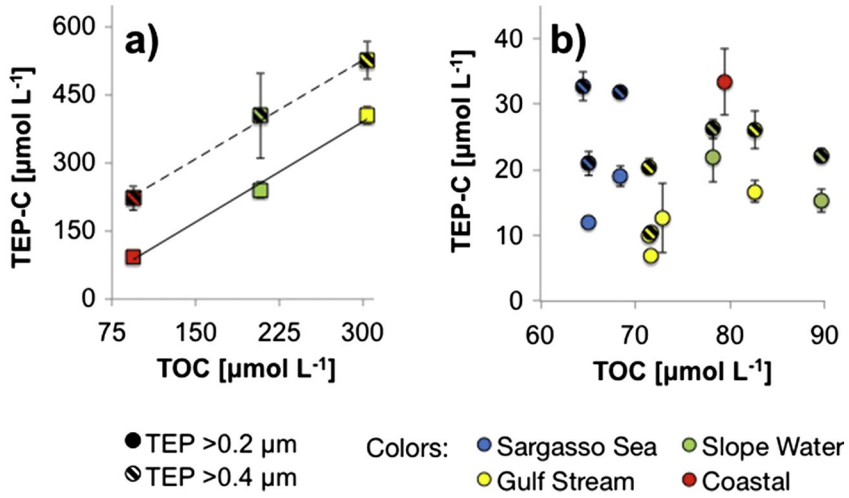

Fig. 7. Correlations of concentrations of TEP-C > 0.4 µm (µmol L^{-1}) (solid symbols) and >0.2 µm (µmol L^{-1}) (striped symbols) with TOC (µmol L^{-1}) in a) SML and b) surface waters. Colors represent sampled areas: Slope Water (green), Gulf Stream (yellow), Sargasso Sea (blue), and Coastal (red). (For interpretation of the references to color in this figure legend, the reader is referred to the web version of this article.)

to escape this cycling in the surface ocean, as well as speculate on temperature, salinity, and wind as physical controls of the environment.

We suggest that the concentration of non-gel organic particles present in surface waters was the primary driver affecting the concentration and vertical distribution of TEP by controlling TEP aggregation and residence time. We present a conceptual framework that explains that TEP is driven to sink out of the SML and surface waters in more productive areas because there are more organic carbon particles to aggregate with TEP and provide ballast (Fig. 9). If there is a greater ratio of organic particles to TEP (such as the phytoplankton bloom in the Slope Water region), then TEP will not accumulate in the SML and may be heavy enough to sink out of the water column, thereby decreasing the TEP residence time (Azetsu-Scott and Passow, 2004; Engel et al., 2004; Mari et al., 2007). If there is a lower concentration of organic particles (such as the oligotrophic subtropical waters), TEP is less likely to sink and will accumulate in the SML and surface waters. The elevated TEP concentrations observed in the surface and upper 100 m in the oligotrophic Sargasso Sea region (Fig. 6) could be explained by a longer residence time of TEP related to lower particle export. This scenario would also explain the higher contribution of larger TEP in the Gulf Stream SML, as a higher fraction of large TEP at higher TEP concentrations is consistent with the idea of self-aggregation of TEP that could be enhanced with longer residence times.

Though we do not have the appropriate measurements to estimate TEP residence times, we use surface POC concentrations as a proxy for particle abundance. The presence of a phytoplankton bloom is identified in the Slope Water region from the elevated Chl-*a*, nutrient and POC concentrations (Fig. 1; Fig. 2f), suggesting that there are probably more particles being exported from that region compared to oligotrophic regions such as the Sargasso Sea. The Slope Water region had the highest average ratio of POC concentration per TEP-C concentration (1.1; expressed as POC/TEP-C in Table 2) in surface waters, while the Gulf Stream region had a ratio of 0.9, and the Sargasso Sea had an even lower ratio of 0.4, indicating that the relative importance of POC with respect to TEP diminished along the TOC gradient (Table 2). The POC/TEP ratio was relatively low in the Coastal region (0.5), which could signify that the residence time of TEP in a coastal system is less influenced by particles, although still subject to high variability from localized processes

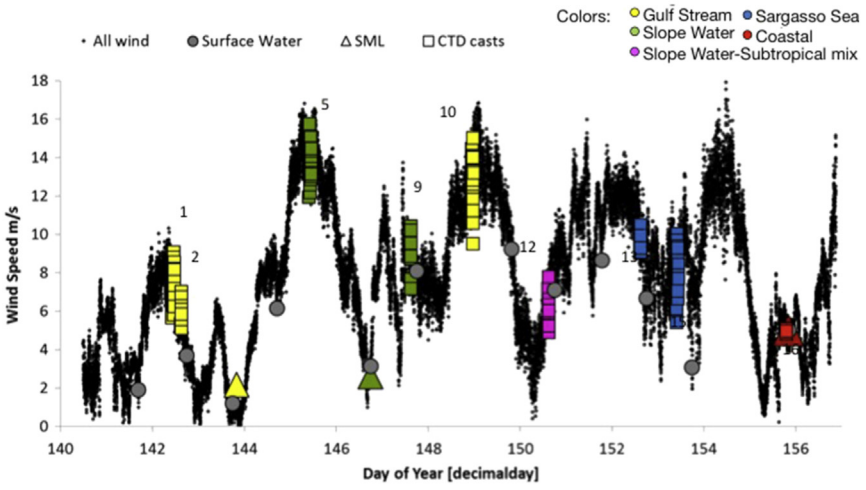

Fig. 8. Wind speed (m s^{-1}) observed during cruise (small black circles). Overlaid symbols indicate wind speed during sampling routines of surface water (large grey circles), SML (triangles) and CTD casts (squares; labeled by cast number). Colors for SML and CTD casts represent sampled areas: Slope Water (green), Gulf Stream (yellow), Slope Water-Subtropical mixture (purple), Sargasso Sea (blue), and Coastal (red). (For interpretation of the references to color in this figure legend, the reader is referred to the web version of this article.)

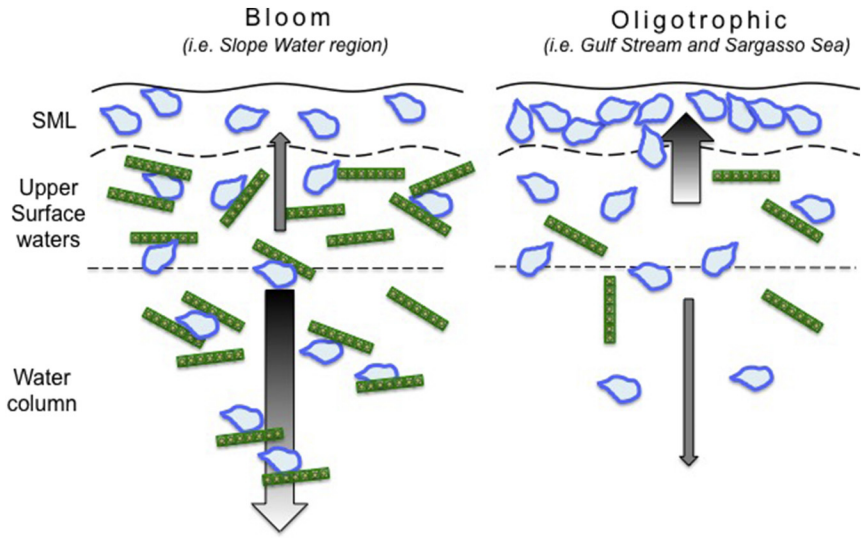

Fig. 9. Conceptual scheme of TEP interactions in marine environments with contrasting productivity and POC concentrations (together indicated by green rectangles) to explain the observed distribution of TEP (blue globules) enrichments in the SML. TEP form heavy particulate aggregates and sink when there are higher concentrations of POC (e.g. bloom conditions), while TEP ascend and accumulate in the SML when POC concentrations are insufficient to ballast TEP (e.g. oligotrophic conditions). (For interpretation of the references to color in this figure legend, the reader is referred to the web version of this article.)

(turbidity, resuspension of sediments, mineral input, and anthropogenic effects) that dictate DOM-POM exchanges (He et al., 2016).

We do not consider wind variation to be significant to this study because our sampling of surface water and SML was biased towards relatively low wind conditions, as all of the SML samples were collected in winds <5 m s^{-1} and surface water samples were collected in winds <10 m s^{-1} (Fig. 8). However, we suspect that the thickness of the Gulf Stream SML, distinguished by a SST ~10 °C warmer than the Slope Water and Coastal regions, was affected by temperature. As the viscosity of water decreases in warmer temperatures, the thickness of the SML should also decrease with increasing temperature (Carlson, 1982; Falkowska, 1999). The greater enrichment of organic material in the Gulf Stream SML is likely partially affected by a decreased SML thickness that presumably helped concentrate organic matter in the SML. In addition, a higher degree of stratification is more likely in the Gulf Stream SML, which would result in slower settling speeds of aggregates (Prairie et al., 2013), further supporting our hypothesis that TEP experiences longer residence time in the Gulf Stream SML.

4.3. Contributions of TEP to global carbon cycle

The elevated contributions of TEP-C to TOC estimated in the SML (Table 3), in combination with the observed relationship between TEP and TOC in the SML (Fig. 7a), suggest that TEP is an important organic constituent of the SML. In each of the regions sampled, TEP-C in the SML represented >100% of the TOC (Table 3), implying that the standard range of conversion factors are not ideal for application to SML samples. There was a larger fraction of TOC estimated as TEP-C in the upper 200 m of the oligotrophic and coastal water columns compared to the Slope Water region. For Slope Water and Gulf Stream surface waters, the contribution of TEP-C to TOC (Table 3) is comparable to the contribution of POC to TOC (Table 2), which suggests that TEP is an important fraction of the POC sampled in those regions.

Similar to our observed TEP and TOC enrichments in the SML, greater organic carbon enrichment was observed in nascent sea spray aerosols (SSA) formed in the Sargasso Sea compared to a region containing higher sea surface Chl-*a* and greater phytoplankton biomass (Quinn et al., 2014). Our data show that the SML of oligotrophic systems have greater TEP and TOC enrichment, which we suggest is the major source of the organic enrichment of SSA. If the processes governing organic enrichment in the SML can be connected to the generation of organically enriched SSA, then there could be an additional sink for surface-active organic matter to consider (Kieber et al., 2016; Long et al., 2011), and an expanded role for TEP in the global carbon cycle (Engel and Galgani, 2016), with greater emphasis on oligotrophic conditions.

5. Summary and conclusion

Throughout the study area, TEP is heavily enriched in the SML relative to underlying surface water (Table 2), and TEP contributes significantly to the organic carbon content of the SML. An organic carbon gradient was observed in the surface waters, with higher TOC, POC, Chl-*a* and TEP concentrations in more productive waters in the northern Slope Water region compared to the more oligotrophic Sargasso Sea or Gulf Stream to the south. A different TOC distribution was observed in overlying SML waters, where appreciably more TOC was concentrated in the less productive areas. The correlation between TEP and TOC in the SML suggests that TEP is a significant component of the organic carbon in this gelatinous interfacial layer. These data suggest that TEP accumulates in the SML in areas where "ballasting" particles heavy enough to carry TEP-particle aggregates downwards are absent (oligotrophic areas). As a consequence, a more pronounced SML, enriched with surface active organic matter, would be expected in oligotrophic regions that are characterized by lower particle export and nutrients than in more productive regions. Future work should trace the production of TEP to its distribution into the SML and upper water column, while controlling the effect of particle abundance on TEP accumulation.

Acknowledgements

We thank the science party and crew aboard *RV Knorr* during the WACS2 field campaign for inclusion and sampling support, especially chief scientist Patricia Quinn. We also thank Amanda Willoughby for sampling support, including POC collection. We thank Theodore Wilson and Wendy Kilthau for collecting and kindly providing the SML samples used in our analyses, and also for contributing useful discussions on the manuscript. We thank Lillian Custals and Wenhao Chen for analyzing TOC and Maria Arroyo for laboratory assistance at RSMAS, as well as Robert Vaillancourt, Jeremiah Stone, and Evan Ntonados at Millersville University for analyzing and providing in situ Chl-*a* data. We thank Julia Sweet for the Alcian Blue calibration. This study was funded by National Science Foundation grant OCE 1436748 to DAH.

References

Alldredge, A.L., Passow, U., Logan, B.E., 1993. The abundance and significance of a class of large, transparent organic particles in the ocean. Deep-Sea Res. I Oceanogr. Res. Pap. 40. http://dx.doi.org/10.1016/0967-0637(93)90129-Q.

Aller, J.Y., Kuznetsova, M.R., Jahns, C.J., Kemp, P.F., 2005. The sea surface microlayer as a source of viral and bacterial enrichment in marine aerosols. J. Aerosol Sci. 36: 801–812. http://dx.doi.org/10.1016/j.jaerosci.2004.10.012.

Azetsu-Scott, K., Passow, U., 2004. Ascending marine particles: significance of transparent exopolymer particles (TEP) in the upper ocean. Limnol. Oceanogr. 49:741–748. http://dx.doi.org/10.4319/lo.2004.49.3.0741.

Bar-Zeev, E., Rahav, E., 2015. Microbial metabolism of transparent exopolymer particles during the summer months along a eutrophic estuary system. Front. Microbiol. 6: 403. http://dx.doi.org/10.3389/fmicb.2015.00403.

Bigg, E.K., Leck, C., 2008. The composition of fragments of bubbles bursting at the ocean surface. J. Geophys. Res. 113, D11209. http://dx.doi.org/10.1029/2007JD009078.

Braman, R.S., Hendrix, S.A., 1989. Nanogram nitrite and nitrate determination in environmental and biological materials by vanadium(III) reduction with chemiluminescence detection. Anal. Chem. 61:2715–2718. http://dx.doi.org/10.1021/ac00199a007.

Burd, A.B., Jackson, G.A., 2009. Particle aggregation. Annu. Rev. Mar. Sci. 1:65–90. http://dx.doi.org/10.1146/annurev.marine.010908.163904.

Burd, A., Buchan, A., Church, M.J., Landry, M.R., McDonnell, A.M.P., Passow, U., Steinberg, D.K., Benway, H.M., 2016. Towards a transformative understanding of the ocean's biological pump: priorities for future research. Report on the NSF Biology of the Biological Pump Workshop. Ocean Carbon and Biogeochemistry (OCB) Program, Woods Hole, MA http://dx.doi.org/10.1575/1912/8263.

Carlson, D.J., 1982. A field evaluation of plate and screen microlayer sampling techniques. Mar. Chem. 11:189–208. http://dx.doi.org/10.1016/0304-4203(82)90015-9.

Carlson, D.J., 1983. Dissolved organic materials in surface microlayers: temporal and spatial variability and relation to sea state. Limnol. Oceanogr. 28:415–431. http://dx.doi.org/10.4319/lo.1983.28.3.0415.

Carlson, C.A., Ducklow, H.W., Hansell, D.A., Smith Jr., W.O., 1998. Organic carbon partitioning during spring phytoplankton blooms in the Ross Sea polynya and the Sargasso Sea. Limnol. Oceanogr. 43, 375–386.

Claquin, P., Probert, I., Lefebvre, S., Veron, B., 2008. Effects of temperature on photosynthetic parameters and TEP production in eight species of marine microalgae. Aquat. Microb. Ecol. 51:1–11. http://dx.doi.org/10.3354/ame01187.

Conan, P., Søndergaard, M., Kragh, T., Thingstad, F., Pujo-Pay, M., Williams, P.J.L.B., Markager, S., Cauwet, G., Borch, N.H., Evans, D., Riemann, B., 2007. Partitioning of organic production in marine plankton communities: the effects of inorganic nutrient ratios and community composition on new dissolved organic matter. Limnol. Oceanogr. 52, 753–765.

Corzo, A., Morillo, J.A., Rodríguez, S., 2000. Production of transparent exopolymer particles (TEP) in cultures of *Chaetoceros calcitrans* under nitrogen limitation. Aquat. Microb. Ecol. 23, 63–72.

Cunliffe, M., Engel, A., Frka, S., Gašparović, B., Guitart, C., Murrell, J.C., Salter, M., Stolle, C., Upstill-Goddard, R., Wurl, O., 2013. Sea surface microlayers: a unified physicochemical and biological perspective of the air-ocean interface. Prog. Oceanogr. 109: 104–116. http://dx.doi.org/10.1016/j.pocean.2012.08.004.

DeMott, P.J., Hill, T.C.J., McCluskey, C.S., Prather, K.A., Collins, D.B., Sullivan, R.C., Ruppel, M.J., Mason, R.H., Irish, V.E., Lee, T., Hwang, C.Y., Rhee, T.S., Snider, J.R., McMeeking, G.R., Dhaniyala, S., Lewis, E.R., Wentzell, J.J.B., Abbatt, J., Lee, C., Sultana, C.M., Ault, A.P., Axson, J.L., Diaz Martinez, M., Venero, I., Santos-Figueroa, G., Stokes, M.D., Deane, G.B., Mayol-Bracero, O.L., Grassian, V.H., Bertram, T.H., Bertram, A.K., Moffett, B.F., Franc, G.D., 2015. Sea spray aerosol as a unique source of ice nucleating particles. Proc. Natl. Acad. Sci. U. S. A. http://dx.doi.org/10.1073/pnas.1514034112.

Dickson, A.G., Sabine, C.L., Christian, J.R., 2007. Guide to Best Practices for Ocean CO_2 Measurements. 3. PICES Spec. Publ.:p. p191. http://dx.doi.org/10.1159/000331784.

Engel, A., 2004. Distribution of transparent exopolymer particles (TEP) in the northeast Atlantic Ocean and their potential significance for aggregation processes. Deep-Sea Res. I Oceanogr. Res. Pap. 51:83–92. http://dx.doi.org/10.1016/j.dsr.2003.09.001.

Engel, A., Galgani, L., 2016. The organic sea-surface microlayer in the upwelling region off the coast of Peru and potential implications for air–sea exchange processes. Biogeosciences 13:989–1007. http://dx.doi.org/10.5194/bg-13-989-2016.

Engel, A., Passow, U., 2001. Carbon and nitrogen content of transparent exopolymer particles (TEP) in relation to their Alcian Blue adsorption. Mar. Ecol. Prog. Ser. 219, 1–10.

Engel, A., Thoms, S., Riebesell, U., Rochelle-Newall, E., Zondervan, I., 2004. Polysaccharide aggregation as a potential sink of marine dissolved organic carbon. Nature 428: 929–932. http://dx.doi.org/10.1038/nature02453.

Falkowska, L., 1999. Sea surface microlayer: a field evaluation of teflon plate, glass plate and screen sampling techniques. Part 2. Dissolved and suspended matter. Oceanologia 41, 223–240.

Filella, M., 2014. Understanding what we are measuring: standards and quantification of natural organic matter. Water Res. 50:287–293. http://dx.doi.org/10.1016/j.watres.2013.12.015.

Grasshoff, K., 1976. Methods of Seawater Analysis. Verlag Chemie, Weinheim and New York.

Hansell, D.A., 2005. Dissolved organic carbon reference material program. EOS Trans. Am. Geophys. Union 86:318. http://dx.doi.org/10.1029/2005EO350003.

He, W., Chen, M., Schlautman, M.A., Hur, J., 2016. Dynamic exchanges between DOM and POM pools in coastal and inland aquatic ecosystems: a review. Sci. Total Environ. 551–552:415–428. http://dx.doi.org/10.1016/j.scitotenv.2016.02.031.

Iversen, M.H., Robert, M.L., 2015. Ballasting effects of smectite on aggregate formation and export from a natural plankton community. Mar. Chem. 175:18–27. http://dx.doi.org/10.1016/j.marchem.2015.04.009.

Jokulsdottir, T., Archer, D., 2016. A stochastic, Lagrangian model of sinking biogenic aggregates in the ocean (SLAMS 1.0): model formulation, validation and sensitivity. Geosci. Model Dev. 9. http://dx.doi.org/10.5194/gmd-9-1455-2016.

Kieber, D.J., Keene, W.C., Frossard, A.A., Long, M.S., Maben, J.R., Russell, L.M., Kinsey, J.D., Tyssebotn, I.M.B., Quinn, P.K., Bates, T.S., 2016. Coupled ocean-atmospheric cycling of marine refractory dissolved organic carbon. Geophys. Res. Lett. n/a-n/a. 10.1002/2016GL068273.

Knulst, J.C., Rosenberger, D., Thompson, B., Paatero, J., 2003. Intensive sea surface microlayer investigations of open leads in the pack ice during Arctic Ocean 2001 expedition. Langmuir 19:10194–10199. http://dx.doi.org/10.1021/la035069+.

Logan, B.E., Passow, U., Alldredge, A.L., Grossartt, H.P., Simont, M., 1995. Rapid formation and sedimentation of large aggregates is predictable from coagulation rates (half-lives) of transparent exopolymer particles (TEP). Deep-Sea Res. II 42, 203–214.

Lomas, M.W., Bates, N.R., 2004. Potential controls on interannual partitioning of organic carbon during the winter/spring phytoplankton bloom at the Bermuda Atlantic time-series study (BATS) site. Deep-Sea Res. I Oceanogr. Res. Pap. 51:1619–1636. http://dx.doi.org/10.1016/j.dsr.2004.06.007.

Long, M.S., Keene, W.C., Kieber, D.J., Erickson, D.J., Maring, H., 2011. A sea-state based source function for size- and composition-resolved marine aerosol production. Atmos. Chem. Phys. 11:1203–1216. http://dx.doi.org/10.5194/acp-11-1203-2011.

Mari, X., Rassoulzadegan, F., Brussaard, C.P.D., Wassmann, P., 2005. Dynamics of transparent exopolymeric particles (TEP) production by *Phaeocystis globosa* under N- or P-limitation: a controlling factor of the retention/export balance. Harmful Algae 4: 895–914. http://dx.doi.org/10.1016/j.hal.2004.12.014.

Mari, X., Rochelle-Newall, E., Torréton, J.-P., Pringault, O., Jouon, A., Migon, C., 2007. Water residence time: a regulatory factor of the DOM to POM transfer efficiency. Limnol. Oceanogr. 52:808–819. http://dx.doi.org/10.4319/lo.2007.52.2.0808.

Mopper, K., Zhou, J., Sri Ramana, K., Passow, U., Dam, H.G., Drapeau, D.T., 1995. The role of surface-active carbohydrates in the flocculation of a diatom bloom in a mesocosm. Deep-Sea Res. II Top. Stud. Oceanogr. 42:47–73. http://dx.doi.org/10.1016/0967-0645(95)00004-A.

Orellana, M.V., Matrai, P.A., Leck, C., Rauschenberg, C.D., Lee, A.M., Coz, E., 2011. Marine microgels as a source of cloud condensation nuclei in the high arctic. Proc. Natl. Acad. Sci. U. S. A. 108, 13612–13617.

Passow, U., 2002a. Transparent exopolymer particles (TEP) in aquatic environments. Prog. Oceanogr. 55, 287–333.

Passow, U., 2002b. Production of transparent exopolymer particles (TEP) by phyto- and bacterioplankton. Mar. Ecol. Prog. Ser. 236:1–12. http://dx.doi.org/10.3354/meps236001.

Passow, U., Alldredge, A.L., 1995. A dye-binding assay for the spectrophotometric measurement of transparent exopolymer particles (TEP). Limnol. Oceanogr. 40, 1326–1335.

Passow, U., Alldredge, A.L., Logan, B.E., 1994. The role of particulate carbohydrate exudates in the flocculation of diatom blooms. Deep-Sea Res. I Oceanogr. Res. Pap. 41:335–357. http://dx.doi.org/10.1016/0967-0637(94)90007-8.

Prairie, J.C., Ziervogel, K., Arnosti, C., Camassa, R., Falcon, C., Khatri, S., McLaughlin, R.M., White, B.L., Yu, S., 2013. Delayed settling of marine snow at sharp density transitions driven by fluid entrainment and diffusion-limited retention. Mar. Ecol. Prog. Ser. 487. http://dx.doi.org/10.3354/meps10387.

Prairie, J.C., Ziervogel, K., Camassa, R., McLaughlin, R.M., White, B.L., Dewald, C., Arnosti, C., 2015. Delayed settling of marine snow: effects of density gradient and particle properties and implications for carbon cycling. Mar. Chem. 175:28–38. http://dx.doi.org/10.1016/j.marchem.2015.04.006.

Quinn, P.K., Bates, T.S., Schulz, K.S., Coffman, D.J., Frossard, A.A., Russell, L.M., Keene, W.C., Kieber, D.J., 2014. Contribution of sea surface carbon pool to organic matter enrichment in sea spray aerosol. Nat. Geosci. 7, 228–232.

Schlitzer, R., 2015. Ocean Data View. odv.awi.de.

Strickland, J.D.H., Parsons, T.R., 1972. A Practical Handbook of Seawater Analysis. second ed. Fisheries Research Board of Canada, Ottawa.

Sun, C.-C., Wang, Y.-S., Li, Q.P., Yue, W.-Z., Wang, Y.-T., Sun, F.-L., Peng, Y.-L., 2012. Distribution characteristics of transparent exopolymer particles in the Pearl River estuary, China. J. Geophys. Res. 117, G00N17. http://dx.doi.org/10.1029/2012jg001951.

Thornton, D.C.O., 2014. Dissolved organic matter (DOM) release by phytoplankton in the contemporary and future ocean. Eur. J. Phycol. 49:20–46. http://dx.doi.org/10.1080/09670262.2013.875596.

Thuy, N.T., Lin, J.C.-T., Juang, Y., Huang, C., 2015. Temporal variation and interaction of full size spectrum Alcian blue stainable materials and water quality parameters in a reservoir. Chemosphere 131:139–148. http://dx.doi.org/10.1016/j.chemosphere.2015.03.023.

Verdugo, P., Alldredge, A.L., Azam, F., Kirchman, D.L., Passow, U., Santschi, P.H., 2004. The oceanic gel phase: a bridge in the DOM-POM continuum. Mar. Chem. 92, 67–85.

Wang, X., Sultana, C.M., Trueblood, J., Hill, T.C.J., Malfatti, F., Lee, C., Laskina, O., Moore, K.A., Beall, C.M., McCluskey, C.S., Cornwell, G.C., Zhou, Y., Cox, J.L., Pendergraft, M.A., Santander, M.V., Bertram, T.H., Cappa, C.D., Azam, F., DeMott, P.J., Grassian, V.H., Prather, K.A., 2015. Microbial control of sea spray aerosol composition: a tale of two blooms. ACS Cent. Sci. 1:124–131. http://dx.doi.org/10.1021/acscentsci.5b00148.

Wanninkhof, R., Feely, R., Millero, F., Curry, R., Hansell, D., Key, R., Swift, J., Smethie, B., Fine, R., Jenkins, B., McNichol, A., D., E., 2013. Carbon Dioxide, Hydrographic, and Chemical Data Obtained During the R/V Atlantis Cruise in the Atlantic Ocean on CLIVAR Repeat Hydrography Section A22 (Mar. 24–Apr. 17, 2012). Oak Ridge, Tennessee. http://dx.doi.org/10.3334/CDIAC/otg.CLIVAR_A22_2012.

Wilson, T.W., Ladino, L.A., Alpert, P.A., Breckels, M.N., Brooks, I.M., Browse, J., Burrows, S.M., Carslaw, K.S., Huffman, J.A., Judd, C., Kilthau, W.P., Mason, R.H., McFiggans, G., Miller, L.A., Nájera, J.J., Polishchuk, E., Rae, S., Schiller, C.L., Si, M., Temprado, J.V., Whale, T.F., Wong, J.P.S., Wurl, O., Yakobi-Hancock, J.D., Abbatt, J.P.D., Aller, J.Y., Bertram, A.K., Knopf, D.A., Murray, B.J., 2015. A marine biogenic source of atmospheric ice-nucleating particles. Nature 525:234–238. http://dx.doi.org/10.1038/nature14986.

Wurl, O., Holmes, M., 2008. The gelatinous nature of the sea-surface microlayer. Mar. Chem. 110:89–97. http://dx.doi.org/10.1016/j.marchem.2008.02.009.
Wurl, O., Miller, L., Röttgers, R., Vagle, S., 2009. The distribution and fate of surface-active substances in the sea-surface microlayer and water column. Mar. Chem. 115:1–9. http://dx.doi.org/10.1016/j.marchem.2009.04.007.
Wurl, O., Miller, L., Vagle, S., 2011a. Production and fate of transparent exopolymer particles in the ocean. J. Geophys. Res. C: Oceans 116.
Wurl, O., Wurl, E., Miller, L., Johnson, K., Vagle, S., 2011b. Formation and global distribution of sea-surface microlayers. Biogeosciences 8:121–135. http://dx.doi.org/10.5194/bg-8-121-2011.
Zetsche, E.-M., Ploug, H., 2015. Marine chemistry special issue: Particles in aquatic environments: From invisible exopolymers to sinking aggregates. Mar. Chem. 175, 1–4.